

A Pragmatic Coded Modulation Scheme for High-Spectral-Efficiency Fiber-Optic Communications

Benjamin P. Smith, Frank R. Kschischang *Fellow, IEEE*

Abstract—A pragmatic coded modulation system is presented that incorporates signal shaping and exploits the excellent performance and efficient high-speed decoding architecture of staircase codes. Reliable communication within 0.62 bits/s/Hz of the estimated capacity (per polarization) of a system with $L = 2000$ km is provided by the proposed system, with an error floor below 10^{-20} . Also, it is shown that digital backpropagation increases the achievable spectral efficiencies—relative to linear equalization—by 0.55 to 0.75 bits/s/Hz per polarization.

Index Terms—Staircase codes, fiber-optic communications, digital backpropagation, forward error correction, coded modulation, channel capacity.

I. INTRODUCTION

RECENT progress has been made in estimating the information-theoretic capacity of the class of fiber-optic communication systems that are (presently) of commercial interest [1], but existing systems perform far from the fundamental limits of the channel. While signal processing and coded modulation techniques promise to eliminate this gap, their implementations—at the speeds present in fiber-optic systems—present significant challenges.

Many existing proposals for coded modulation in fiber-optic communication systems amount to using techniques currently used in electrical wireline and wireless communication systems. For example, in [2], the authors propose a concatenated coding system with inner trellis-coded modulation (for an 8-PSK constellation) and an outer product-like code, and in [3]–[5], the authors propose using low-density parity-check (LDPC) codes for coded modulation. In both cases, the proposals are verified by simulation, where the channel is assumed to be a classical additive white Gaussian noise (AWGN), but no consideration is given to the real-world implementation challenges for the proposed systems.

Other proposals for coded modulation in fiber-optic systems consider simplified channel models, and design codes for the resulting systems. For example, in [6], the authors design a trellis-coded polarization-shift-keying modulation system, but their channel model only considers laser phase noise, i.e., effects related to the propagation over fiber are completely ignored. In [7], the authors consider a nonlinear phase noise channel model studied by [8], and design a multi-level

coded modulation system with Reed-Solomon codes at each level. However, this channel model assumes a single-channel dispersion-less system, which is not of practical interest.

In this paper, we take a pragmatic approach to coded modulation for fiber-optic systems, that addresses the deficiencies of the aforementioned proposals. Due to the fact that product-like codes with syndrome-based decoding have efficient high-speed decoders [9], we consider systems with hard-decision decoding. Furthermore, the channel model for which the codes are designed is not a simplified one, but rather is derived from (computationally intensive) simulations of the fiber-optic systems based on the generalized nonlinear Schrödinger (GNLS) equation [(1), below], and thus accurately models the non-AWGN channel that occurs in optical communication systems.

In contrast to most classically studied communication channels, optical fiber exhibits significant nonlinearity (in the intensity of the guided light) [10]. Furthermore, amplification acts as a source of distributed AWGN, and fiber chromatic dispersion acts as a distributed linear filter. Complicating matters, these three fundamental effects *interact* over the length of transmission. In [1], signal processing is performed via digital backpropagation, in order to attempt to compensate the channel impairments. However, their results do not quantify the benefits of this compensation strategy. Since digital backpropagation is computationally expensive, one approach to reducing the computational burden is to increase the step-size of the algorithm, as in [11], [12]. In this paper, we compare the achievable rates for two extreme cases: digital backpropagation (as in [1]), and a linear equalizer (which can be considered as a form of “linear backpropagation” in which the step-size is the system’s length).

In Section II, we review staircase codes, the system model for a fiber-optic communication system, and digital backpropagation. In Section III, we compare the transmission rates that can be achieved using digital backpropagation with those achievable by linear equalization. In Section IV, we present the details of a pragmatic coded modulation system, and compare the performance of the system to the capacity estimates.

II. PRELIMINARIES

A. Staircase Codes

Staircase codes [9] are a family of high-rate binary error-correcting codes suitable for high-speed fiber-optic communications. Staircase codes can be interpreted as *generalized*

Benjamin P. Smith and Frank R. Kschischang are with the Electrical and Computer Engineering Department, University of Toronto, 10 King’s College Road, Toronto, Ontario M5S 3G4, Canada (e-mail: {ben, frank}@comm.utoronto.ca).

LDPC codes, that is, sparse graph-based codes whose constraint nodes are error-correcting codes, not the single-parity-check error-detecting codes used in the constraint nodes of conventional LDPC codes. With such generalized LDPC codes, algebraic decoding can be applied at the constraint nodes, and the decoder can operate exclusively on syndromes. As discussed in [9], this significantly reduces the decoder data-flow (relative to a message-passing LDPC decoder), admitting an efficient high-speed implementation. Furthermore, due to the error correcting capabilities of the constraint nodes, staircase codes have very low error floors, which can be estimated analytically. Finally, due to their structural properties, staircase codes provide superior performance to product codes.

Staircase codes are completely characterized by the relationship between successive matrices of symbols. Specifically, consider the (infinite) sequence B_0, B_1, B_2, \dots of m -by- m matrices B_i , $i \in \mathbb{Z}^+$. Block B_0 is initialized to a reference state known to the encoder-decoder pair, e.g., block B_0 could be initialized to the all-zeros state, i.e., an m -by- m array of zero symbols. Furthermore, we select a conventional FEC code (e.g., Hamming, BCH, Reed-Solomon, etc.) in systematic form to serve as the *component* code; this code, which we henceforth refer to as C , is selected to have blocklength $2m$ symbols, r of which are parity symbols.

Generally, the relationship between successive blocks in a staircase code satisfies the following relation: for any $i \geq 1$, each of the rows of the matrix $[B_{i-1}^T B_i]$ is a valid codeword in C . Just as in a conventional product code, any given symbol in any given block B_i participates in two constraints: one to satisfy the condition that each row of $[B_{i-1}^T B_i]$ is a codeword of C , and one to satisfy the condition that each row of $[B_i^T B_{i+1}]$ is a codeword of C .

B. System Model

We consider a coherent fiber-optic communication system. Between the transmitter and receiver, standard-single-mode fiber and ideal distributed Raman amplification are assumed, but we note that the methods presented herein also apply to alternate system configurations (e.g., systems with inline dispersion-compensating fiber, and/or lumped amplification). The complex baseband representation of the signal in a single polarization at the output of the transmitter is $A(0, t)$, and at the input of the receiver is $A(L, t)$, where L is the total system length; note that $A(z, t)$ represents the full field, i.e., in general it represents co-propagating dense wavelength-division-multiplexed signals.

The generalized non-linear Schrödinger (GNLS) equation expresses the evolution of $A(z, t)$:

$$\frac{\partial A}{\partial z} + \frac{j\beta_2}{2} \frac{\partial^2 A}{\partial t^2} - j\gamma |A|^2 A = n(z, t). \quad (1)$$

Since ideal distributed Raman amplification is assumed, the loss term has been omitted, and $n(z, t)$ is a circularly symmetric complex Gaussian noise process with autocorrelation

$$\mathcal{E}[n(z, t)n^*(z', t')] = \alpha h v_s K_T \delta(z - z', t - t'),$$

where h is Planck's constant, v_s is the optical frequency, and K_T is the phonon occupancy factor. In Table I, we provide parameter values for the system components.

TABLE I
SYSTEM PARAMETER VALUES

| | |
|-----------------------------------|--|
| Second-order dispersion β_2 | -21.668 ps ² /km |
| Loss α | 4.605×10^{-5} m ⁻¹ |
| Nonlinear coefficient γ | 1.27 W ⁻¹ km ⁻¹ |
| Center carrier frequency v_s | 193.41 THz |
| Phonon occupancy factor K_T | 1.13 |

Note that the scalar equation (1)—whose numerical solution is used to generate all of the results of this paper—governs propagation of waveforms in a single polarization mode. The achievable rates for a dual-polarized transmission system would be approximately (but slightly less than) twice as large as for the single polarization system considered here, but a more complicated vector version of (1), taking into account the effects of fiber birefringence and coupling between the polarization modes as well as the stochastic nature of polarization mode dispersion, would need to be considered.

C. Digital Backpropagation

Throughout propagation over an optical fiber, stochastic effects (noise), linear effects (dispersion) and nonlinear effects (Kerr nonlinearity) *interact*, and—even in the absence of noise—solving the GNLS equation requires numerical techniques. On the other hand, in the absence of noise, the system is invertible, i.e., the transmitted signal $A(0, t)$ can be recovered from the received signal $A(NL_A)$ by inverting the channel. When the channel is inverted by digital signal processing, we say the receiver performs *digital backpropagation*.

The most commonly used numerical method to solve the GNLS equation is the split-step Fourier method [13], [14]. The basic idea is to divide the total fiber length into short segments, then to consider each segment as the concatenation of (separable) nonlinear and linear transforms (for distributed amplification, an additive noise is added after the linear step). In the following, we briefly review the split-step Fourier method. For simplicity of the presentation, we ignore the effects of amplification, which can be incorporated into a numerical solver in an obvious manner.

For a known $A(z = z_0, t)$, the split-step Fourier method calculates $A(z = z_0 + h, t)$ as follows. First, in the absence of linear effects, the GNLS equation has the form,

$$\frac{\partial A}{\partial z} = j\gamma |A|^2 A,$$

with solution,

$$A(z = z_0 + h, t) = A(z = z_0, t) \exp(j\gamma |A(z = z_0, t)|^2 h).$$

We now use this solution as the input to the the linear step, i.e., let

$$\hat{A}(z = z_0, t) = A(z = z_0, t) \exp(j\gamma |A(z = z_0, t)|^2 h)$$

be the input to the linear step. The linear form of the GNLS equation is

$$\frac{\partial A}{\partial z} = -\frac{\alpha}{2} A - \frac{j\beta_2}{2} \frac{\partial^2 A}{\partial t^2},$$

which can be efficiently solved in the frequency domain. Defining

$$A(z, t) = \frac{1}{2\pi} \int_{-\infty}^{\infty} \tilde{A}(z, \omega) \exp(j\omega t) d\omega,$$

it can be shown that

$$\tilde{A}(z = z_0 + h, \omega) = \tilde{A}(z = z_0, \omega) \exp \left(\left(j \frac{\beta_2}{2} \omega^2 - \frac{\alpha}{2} \right) h \right). \quad (2)$$

Putting this together, we have

$$A(z = z_0 + h, t) = \mathcal{F}^{-1} \left\{ \mathcal{F} \left\{ \hat{A}(z = z_0, t) \right\} \cdot \exp \left(\left(j \frac{\beta_2}{2} \omega^2 - \frac{\alpha}{2} \right) h \right) \right\},$$

where \mathcal{F} is the Fourier transform operator.

Digital backpropagation is then accomplished by the split-step Fourier method, using a negative step-size h . Note that, in general, $A(z, t)$ is the complex envelope of a multi-channel optical signal. It follows that *full compensation* of channel impairments—even if only a single channel is of interest to the receiver—requires backpropagation to be performed on the *multi-channel* signal, since nonlinearity induces interaction between signal components at non-overlapping frequencies. However, in practice, receivers operate on a per-channel basis. Even if a multi-channel receiver were available, co-propagating channels may be optically-routed in or out throughout transmission, and thus channels that have co-propagated with the desired channel may not even be available at the receiver (and those channels that are available may not have co-propagated with the desired channel). Therefore, we consider single-channel backpropagation, in which the receiver first extracts the channel of interest from $A(z = L, t)$ (via a bandpass filter), and performs digital backpropagation on the corresponding signal.

III. ACHIEVABLE RATES

Although many current state-of-the-art systems include some form of electronic dispersion compensation (i.e., equalization) in the receiver, digital backpropagation is significantly more computationally intensive, since many steps—each of which has roughly the complexity of a standard equalization scheme—of the split-step Fourier method are required to accurately compensate the nonlinear effects.

In this section we compare the achievable information rates when (only) linear equalization is performed to the achievable rates of a system that performs digital backpropagation. Furthermore, the resulting capacity estimates serve as upper bounds on the performance of a coded modulation system, the design of which we consider in Section IV.

A. Memoryless Capacity Estimation

In [1], Essiambre et al. present an estimate of the information theoretic capacity of optical fiber networks. In this section, we review their technique, which we will make use of in the following.

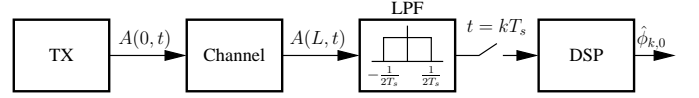


Fig. 1. System model for memoryless capacity evaluation

1) *Transmitter*: We consider a system that employs pulse-amplitude modulation (PAM) with (orthonormal) sinc pulses. That is, the transmitted signal (corresponding to the baseband representation of the l -th channel) is of the form

$$X_l(t) = \sum_{k=-\infty}^{\infty} \frac{\phi_{k,l}}{\sqrt{T_s}} \text{sinc} \left(\frac{t - kT_s}{T_s} \right),$$

where $\text{sinc}(\theta) = \frac{\sin \pi \theta}{\pi \theta}$. The $\phi_{k,l}$ are elements of a discrete-amplitude continuous-phase input constellation \mathcal{M} , i.e. for N rings, $\theta \in [0, 2\pi)$, and $r \geq 0$,

$$\mathcal{M} = \{m \cdot r \exp(j\theta) \mid m \in \{1, 2, \dots, N\}\}.$$

Each ring is assumed equiprobable, and for a given ring, the phase distribution is uniform. This choice of constellation is motivated by the fact that the channel represented by the GNLS equation can be argued to be statistically rotationally invariant (i.e., for a channel with conditional distribution $f(y|x)$, $f(y|x_0) = f(y \exp(j\theta) | x_0 \exp(j\theta))$ for $\theta \in [0, 2\pi)$) and thus points on the same ring can be considered “equivalent”, which reduces the computational requirements in characterizing the channel. Furthermore, it is well known that, for sufficiently many rings, the Shannon Limit of the AWGN channel can be closely approached, and one would expect this to be true also for the non-AWGN channel considered here.

In the general case of a multi-channel system having $2B+1$ channels with a channel spacing $1/T_s$ Hz, the input to the fiber has the form

$$A(z = 0, t) = \sum_{k=-\infty}^{\infty} \sum_{l=-B}^B \frac{\phi_{k,l}}{\sqrt{T_s}} \text{sinc} \left(\frac{t - kT_s}{T_s} \right) e^{j2\pi l t / T_s}.$$

2) *Receiver*: By convention, the channel of interest (COI) is assumed to correspond to $l = 0$. From the channel output $A(L, t)$, the (baseband) digital coherent optical receiver extracts the COI via an ideal low-pass filter, and the corresponding signal is sampled at the rate $1/T_s$. The resulting discrete-time signal is then compensated by digital signal processing, i.e., backpropagation (BP) or linear equalization (EQ), providing estimates $\hat{\phi}_{k,0}$ of the transmitted symbols $\phi_{k,0}$, as illustrated in Fig 1.

3) *Channel Model*: In order to facilitate the capacity estimation, the discrete-time channel is assumed to be *memoryless*, i.e., it is assumed that backpropagation removes any dependence (introduced by the channel) between received symbols. The (memoryless) conditional distribution of the channel is estimated from numerical simulations.

Since the channel is statistically rotationally invariant, observations of transmitted points from the same ring are first ‘back-rotated’ to the real axis, as illustrated in Fig. 2. The back-rotated points are represented by $\tilde{\phi}_{k,l}$,

$$\tilde{\phi}_{k,l} = \hat{\phi}_{k,l} \exp(-j(\Phi_{\text{XPM}} + \angle \phi_{k,l})),$$

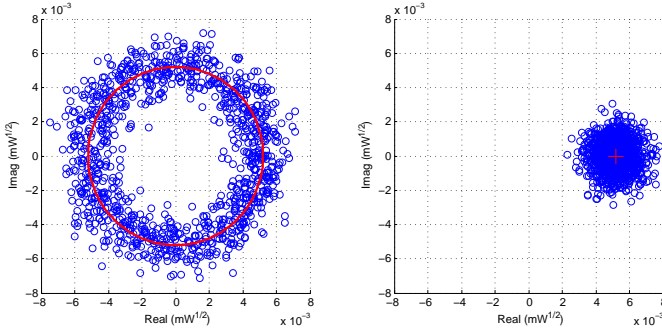


Fig. 2. Channel outputs for a fixed-ring input, and back-rotated outputs.

where Φ_{XPM} is a constant (input-independent) phase rotation contributed by cross-phase modulation (XPM).

Next, for each i and a fixed l (the channel of interest), we calculate the mean μ_i and covariance matrix Ω_i (of the real and imaginary components) of those $\hat{\phi}_{k,l}$ corresponding to the i -th ring, and model the distribution of those $\hat{\phi}_{k,l}$ by $\mathcal{N}(\mu_i, \Omega_i)$. Finally, from the rotational invariance of the channel, the channel is modeled as

$$f(y|x = r \cdot i \exp(j\phi)) \sim \mathcal{N}(\mu_i \exp(j\phi), \Omega_i),$$

where the (constant) phase rotation due to Φ_{XPM} is ignored, since it can be canceled in the receiver. Note that this model reduces to an additive ‘noise’ model when $\mu_i = (r \cdot i, 0)$, but in general this relationship need not be true.

4) *Capacity Estimation*: The mutual information of the memoryless channel is

$$I(X; Y) = \iint f(x, y) \log_2 \frac{f(y|x)}{f(y)} dx dy,$$

where $f(x)$ represents the input distribution on \mathcal{M} with equiprobable rings and a uniform phase distribution, which provides an estimate of the capacity of an optically-routed fiber-optic communication system.

5) *Signaling Parameters*: In Table II we provide the parameters of the signaling scheme, to be used throughout the remainder of this work. In general, further increasing the number of simulated channels has a negligible effect on the capacity estimates.

TABLE II
SIGNALING PARAMETER VALUES

| | |
|-----------------------|--------------|
| Baud rate $1/T_s$ | 100 GHz |
| Channel bandwidth W | 101 GHz |
| Number of rings N | 64 |
| Number of channels | $2B + 1 = 5$ |

B. Results

In Fig. 3, we present the achievable spectral efficiencies. We consider systems of length $L = 500, 1000$ and 2000 km. The signal-to-noise ratio (SNR) is defined as

$$\text{SNR} = \frac{P}{N_{\text{ASE}} W},$$

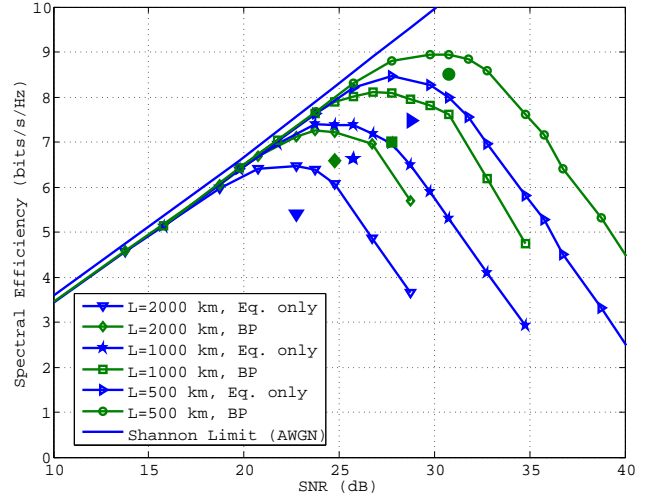


Fig. 3. (Theoretically) achievable spectral efficiencies for BP and EQ at different transmission lengths. Also shown (by the isolated symbols) are the spectral efficiencies achieved by the staircase-coded systems described in Table IV.

where P is the average transmitter power, W is the bandwidth occupied by a single channel, and $N_{\text{ASE}} = L \alpha h \nu_s K_T$ is the power spectral density of the noise. In contrast to conventional linear Gaussian channel models, N_{ASE} is fixed by the choices of L and the amplification technique. Therefore, for a fixed system, the SNR can be increased only by increasing the input power.

For $L = 2000$ km, the peak spectral efficiency is approximately 6.45 bits/s/Hz per polarization when only linear equalization is performed, but increases to approximately 7.2 bits/s/Hz per polarization for digital backpropagation. For $L = 1000$ km, the peak spectral efficiency is approximately 7.4 bits/s/Hz per polarization when only linear equalization is performed, but increases to approximately 8.1 bits/s/Hz per polarization for digital backpropagation. Finally, for $L = 500$ km, the peak spectral efficiency is approximately 8.45 bits/s/Hz per polarization when only linear equalization is performed, but increases to approximately 9.0 bits/s/Hz per polarization for digital backpropagation.

For the cases considered, digital backpropagation increases the achievable spectral efficiencies—relative to linear equalization—by 0.55 to 0.75 bits/s/Hz per polarization. From the standpoint of achievable rates, the channel is “nearly” linear for most input powers of interest, in the sense that linear equalization achieves rates that closely approach those achievable via backpropagation. Furthermore, even when the input power is such that the achievable rate is maximized, the distortion introduced by the channel is well-modeled as AWGN, and thus classical coding methods ought to provide near-capacity reliable communications. However, due to the extremely high per-channel data rates of fiber-optic systems, implementation challenges arise. In the following, we propose a pragmatic coded modulation system—based on staircase codes—that provides excellent performance and an efficient high-speed implementation.

IV. A PRAGMATIC CODED-MODULATION SCHEME

Although staircase codes are binary error-correcting codes with a syndrome-based decoding algorithm, they can be adapted—via known techniques—to provide error-correction in high-spectral-efficiency communication systems, while maintaining their efficient decoding architecture. In the following, we first review these techniques, then we provide the parameters of staircase-coded systems and present their performance.

A. Coding

For high-spectral-efficiency communications, the set of channel input symbols (i.e., the modulation constellation) must be sufficiently large, and coding is required on the resulting non-binary input alphabet. At first glance, this would seem to require the design of error-correction codes over non-binary alphabets, with a decoding algorithm that accounts for the distance metric implied by the underlying channel. Indeed, this ‘direct’ approach provides motivation for trellis-coded modulation [15], in which the code is designed to optimize the minimum Euclidean distance between transmitted sequences.

Alternatively, by considering the set of channels induced by the bit-labels of the constellation points, coded modulation via binary codes can be applied with—in principle—no loss of optimality. To see this, consider a 2^M -point constellation \mathcal{A} , for which each symbol is labeled with a unique binary M -tuple (b_1, b_2, \dots, b_M) . For a channel with input $X \in \mathcal{A}$, and an output Y , the capacity of the resulting channel is $I(X; Y)$ (maximized over the input distribution $p(x)$), which can be expanded by the chain rule of mutual information:

$$\begin{aligned} I(X; Y) &= I(b_1, b_2, \dots, b_M; Y) \\ &= I(b_1; Y) + I(b_2; Y|b_1) + \dots + \\ &\quad I(b_M; Y|b_1, b_2, \dots, b_{M-1}) \end{aligned} \quad (3)$$

Note that each term (i.e., the sub-channels) in the expansion defines a binary-input channel, for which binary error-correction codes—such as staircase codes—can be applied; this approach is referred to as multi-level coding (MLC) [16]. Furthermore, if a capacity-approaching code is applied to each sub-channel, then the capacity of the modulation scheme is achieved, that is, there is no loss in optimality in applying binary coding to each sub-channel. However, from (3), it is implied that decoding is performed in stages, since decoded bits from lower-indexed levels provide side information for decoding higher levels; the resulting decoding architecture is referred to as a multi-stage decoder.

Note that the multi-stage architecture introduces decoding latency to the higher levels, requires memory to store channel outputs prior to decoding (since outputs are ‘held’ until decoded bits from the lower levels are available), and requires an individual code for each sub-channel. Clearly, the latency and memory issues can be eliminated simply by ignoring the conditioning in (3), and the resulting system has capacity

$$C_{\text{PID}} = I(b_1; Y) + I(b_2; Y) + \dots + I(b_M; Y),$$

where PID stands for “parallel independent decoding”. However, even when capacity-achieving codes (i.e., with rates

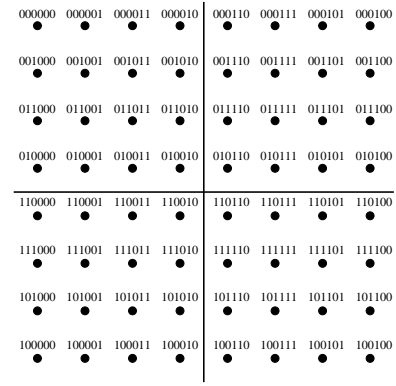


Fig. 4. A Gray-labeled 64-QAM constellation.

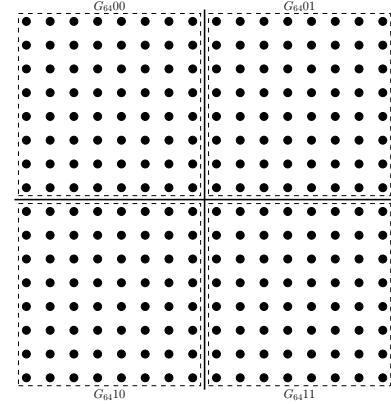


Fig. 5. A mixed-labeled 256-QAM constellation, where G_{64} represents a Gray-labeled 64-QAM constellation.

$I(b_i; Y)$) are applied to each sub-channel, C_{PID} may be significantly less than $I(X; Y)$. Note that the capacities of the individual bit-channels depend on the constellation labeling; for MLC their overall sum is fixed, regardless of the labeling, but for PID their sum (i.e., C_{PID}) depends on the labeling. In fact, for Gray-labeling¹ (see Fig. 4), the difference between C_{PID} and $I(X; Y)$ essentially vanishes, as shown in [17]. Furthermore, even though the capacities of the individual sub-channels are not identical, a single binary error-correcting code (whose rate is the average of the bit-channel rates) provides near-capacity performance, which addresses the third issue with MLC; this approach is referred to as bit-interleaved coded modulation (BICM).

B. Shaping

Implicit in the definition of channel capacity is an optimization over the input alphabet of the channel. For example, the optimal input distribution for the additive white Gaussian noise channel is itself Gaussian. Indeed, the ring-like constellations used in Section III provide shaping gain relative to a QAM-like constellation. In order to approach the capacity estimates of the fiber optic channel, shaping is essential in any coded modulation scheme.

¹A Gray-labeling has the property that the binary M -tuples of nearest neighbor constellation points differ in only a single position

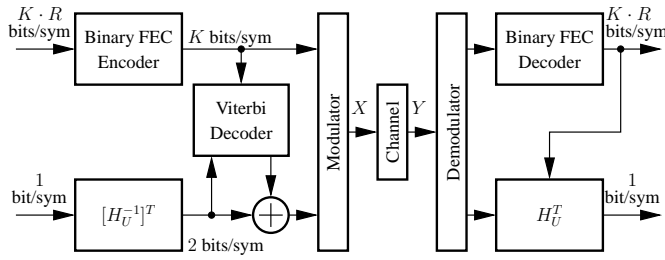


Fig. 6. The coded modulation system with shaping.

In the following, we describe an adaptation of trellis shaping [18] to a bit-interleaved coded modulation system. Consider the bit-labeling in Fig. 5. For each point in a given quadrant, the two most significant bits are the same; we refer to these two bits as the *shaping* bits. Furthermore, by the chain rule of mutual information, we have

$$\begin{aligned} I(X; Y) &= I(b_1, b_2, \dots, b_K, b_{K+1}, b_{K+2}; Y) \\ &= \underbrace{I(b_1, b_2, \dots, b_K; Y)}_{K \cdot R} \\ &\quad + \underbrace{I(b_{K+1}, b_{K+2}; Y | b_1, b_2, \dots, b_K)}_1, \end{aligned} \quad (4)$$

which provides a ‘two’-level (i.e., an MLC scheme with two generalized levels) interpretation of the proposed system, with $M = K + 2$. The first term in (4) represents the lowest level, to which error-correction coding is applied; for the reasons stated previously, we will use bit-interleaved coded modulation at this level. If the rate of the error-correcting code is R , then this term communicates $K \cdot R$ bits per symbol. The second term, the upper-level of the pseudo-MLC scheme, is responsible for providing shaping. In trellis shaping, this is provided by communicating—via (b_{K+1}, b_{K+2}) —a single bit per symbol, while using a Viterbi-based shaping algorithm to select the remaining bit (of freedom) to produce a sequence of symbols with a (nearly) bi-dimensional Gaussian distribution. Intuitively, the bi-dimensional Gaussian distribution results from two facts: the Viterbi search selects the signal path that minimizes energy, and for a fixed entropy, the Gaussian distribution is the minimum energy distribution.

As in [18], the Viterbi algorithm operates on the trellis of a four-state convolutional code C_U with generator matrix $G_U = [1 + D^2, 1 + D + D^2]$ and syndrome-former matrix $H_U^T = [1 + D + D^2, 1 + D^2]^T$. The overall operation of the system is as illustrated in Fig. 6.

C. Pragmatic Coded-Modulation via Staircase Codes

To further reduce the complexity of the coded modulation system, we focus on systems for which the error-correcting code (at the lowest level) is decoded by a hard-decision decoder that receives hard decisions from the channel. That is, the demodulator in Fig. 6 outputs K bits (the b_1, b_2, \dots, b_K corresponding to the constellation point closest to the received symbol) to the FEC decoder for every received symbol; we assume coding is applied to these bits via BICM, and refer to such a system as a ‘pragmatic’ coded-modulation system.

TABLE III
ACHIEVABLE RATES PER POLARIZATION FOR PRAGMATIC
CODED-MODULATION SYSTEM

| Fiber System | K | p_{avg} | P_{in} (dBm) | I_P (bits/s/Hz) |
|-------------------|-----|-----------------------|--------------------------|----------------------|
| $L = 500$ km, EQ | 8 | 1.61×10^{-2} | -6 | 8.05 |
| $L = 500$ km, BP | 8 | 3.52×10^{-3} | -4 | 8.73 |
| $L = 1000$ km, EQ | 6 | 3.88×10^{-3} | -6 | 6.78 |
| $L = 1000$ km, BP | 8 | 2.22×10^{-2} | -4 | 7.77 |
| $L = 2000$ km, EQ | 6 | 2.52×10^{-2} | -6 | 5.98 |
| $L = 2000$ km, BP | 6 | 5.16×10^{-3} | -4 | 6.72 |

In a manner similar to that applied for the capacity estimates in Fig. 3, the achievable rates of the pragmatic coded-modulation system can be estimated via numerical simulations. Since BICM and hard-decision quantization are performed at the lowest level, the capacity of the resulting level is

$$K(1 - H_2(p_{\text{avg}})),$$

where p_{avg} is the average error rate of the received bits at the lowest level, and $H_2(x) = -x \log_2 x - (1 - x) \log_2 (1 - x)$ is the binary entropy function. Furthermore, the highest level communicates exactly 1 bit of information per symbol, and the maximum achievable information rate for the pragmatic system is thus

$$I_P = 1 + K(1 - H_2(p_{\text{avg}})).$$

In Table III, the estimated values of I_P are presented, based on numerical simulations of the systems; in each case, K and the average input power P_{in} are optimized to maximize I_P .

Note that for $L = 2000$ km, the pragmatic coded modulations system has a capacity within 0.47 bits/s/Hz per polarization of the peak spectral efficiency when only linear equalization is performed, and within 0.48 bits/s/Hz per polarization for digital backpropagation. For $L = 1000$ km, the pragmatic coded modulations system has a capacity within 0.62 bits/s/Hz per polarization of the peak spectral efficiency when only linear equalization is performed, and within 0.43 bits/s/Hz per polarization for digital backpropagation. Finally, for $L = 500$ km, the pragmatic coded modulations system has a capacity within 0.40 bits/s/Hz per polarization of the peak spectral efficiency when only linear equalization is performed, and within 0.27 bits/s/Hz per polarization for digital backpropagation. In each case, the dominant contribution to the gap in performance is a result of the hard quantization applied at the lowest level of the (two-level) coded system. Even though the hard quantization scheme leads to some loss in performance, it is directly compatible with the syndrome-based decoding of staircase codes.

We now consider the design of staircase codes for use in the pragmatic coded system. In [9], a G.709-compliant staircase code was presented, with $R = 239/255$, suitable for providing error-correction on a binary symmetric channel with $p \leq 4.8 \times 10^{-3}$. This code is thus suitable for providing error-correction for the linearly-equalized system with $L = 1000$ km and the digitally-backpropagated system with $L = 500$ km. For the other systems, we designed new staircase codes, the parameters of which—including the net coding gain (NCG)—

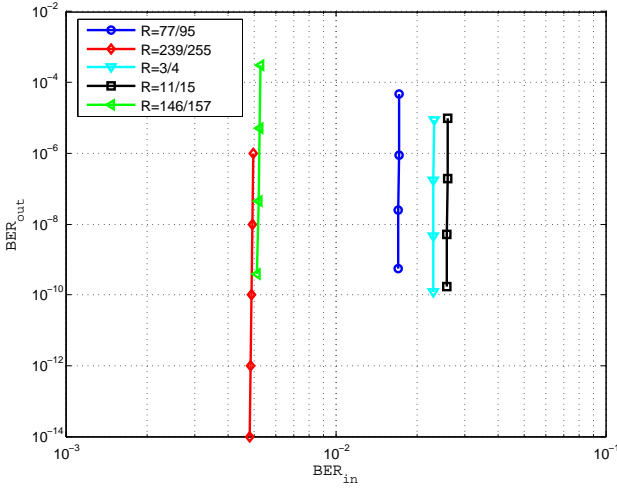


Fig. 7. Performance curves for the staircase codes in Table IV.

are provided in Table IV; the terminology used to describe the codes follows that of Section II-A.

In each case, the length of the (mother) BCH component code is the smallest $2^n - 1$ that is greater than or equal to $2m$.

In Fig. 7, the bit-error-rate curves are plotted. Since these curves (other than the G.709-compliant staircase code) were computed without a hardware implementation, we were only able to obtain results to approximately 10^{-10} . By the error floor estimation methods outlined in [9] (with p set to the average of the sub-channel error rates), none of the systems have error floors above 10^{-20} . Thus, extrapolating the curves to 10^{-15} , each code has been designed to provide an output error rate of better than 10^{-15} at the input error rate induced by its corresponding system.

In Fig. 3, the performance of the staircase coded systems is plotted (the filled symbols), in addition to the estimated capacity curves (the unfilled symbols). For $L = 2000$ km, the system performs within 1.05 bits/s/Hz per polarization of the peak spectral efficiency when only linear equalization is performed, and within 0.62 bits/s/Hz per polarization for digital backpropagation. For $L = 1000$ km, the system performs within 0.78 bits/s/Hz per polarization of the peak spectral efficiency when only linear equalization is performed, and within 1.2 bits/s/Hz per polarization for digital backpropagation. Finally, for $L = 500$ km, the system performs within 0.97 bits/s/Hz per polarization of the peak spectral efficiency when only linear equalization is performed, and within 0.50 bits/s/Hz per polarization for digital backpropagation.

Note that the performance gap increases as the rate of the staircase code (and corresponding sub-channel capacity) decreases, since staircase codes perform closest to capacity at high rates. The performance of those systems could be improved by choosing a multi-dimensional constellation that induces a higher rate (average) sub-channel.

V. CONCLUSIONS

We showed that digital backpropagation increases the achievable spectral efficiencies—relative to linear equalization—by 0.55 to 0.75 bits/s/Hz per polarization.

TABLE IV
STAIRCASE CODES FOR PRAGMATIC CODED SYSTEMS

| Fiber System | m | t | R | NCG (dB) | Spec. Eff. (bits/s/Hz) |
|-------------------|-----|-----|---------|----------|------------------------|
| $L = 500$ km, EQ | 190 | 4 | 77/95 | 10.47 | 7.48 |
| $L = 500$ km, BP | 255 | 3 | 239/255 | 9.41 | 8.50 |
| $L = 1000$ km, EQ | 255 | 3 | 239/255 | 9.41 | 6.62 |
| $L = 1000$ km, BP | 144 | 4 | 3/4 | 10.68 | 7.00 |
| $L = 2000$ km, EQ | 120 | 4 | 11/15 | 10.62 | 5.40 |
| $L = 2000$ km, BP | 628 | 4 | 146/157 | 9.50 | 6.58 |

We proposed a pragmatic coded modulation system that incorporates signal shaping and exploits the excellent performance and efficient high-speed decoding architecture of staircase codes. Reliable communication within 0.62 bits/s/Hz per polarization of the estimated capacity of a system with $L = 2000$ km is provided by the proposed system, with an error floor below 10^{-20} .

REFERENCES

- [1] R.-J. Essiambre, G. Kramer, P. J. Winzer, G. J. Foschini, and B. Goebel, "Capacity limits of optical fiber networks," *J. Lightw. Technol.*, vol. 28, no. 4, pp. 662–701, Sept./Oct. 2010.
- [2] M. Magarini *et al.*, "Concatenated coded modulation for optical communication systems," *IEEE Photon. Technol. Lett.*, vol. 22, no. 16, pp. 1244–1246, Aug. 2010.
- [3] M. Arabaci, I. B. Djordjevic, R. Saunders, and R. M. M. Marcocchia, "Non-binary quasi-cyclic LDPC based coded modulation for beyond 100 Gb/s transmission," *IEEE Photon. Technol. Lett.*, vol. 22, no. 6, pp. 434–436, Mar. 2010.
- [4] I. B. Djordjevic, M. Cvijetic, L. Xu, and T. Wang, "Using LDPC-coded modulation and coherent detection for ultra high-speed optical transmission," *J. Lightw. Technol.*, vol. 25, pp. 3619–3625, Nov. 2007.
- [5] B. P. Smith and F. R. Kschischang, "Future prospects for FEC in fiber-optic communications," *IEEE J. Sel. Topics Quantum Electron.*, vol. 16, no. 5, pp. 1245–1257, Sept./Oct. 2010.
- [6] S. Benedetto, G. Olmo, and P. Poggiolini, "Trellis coded polarization shift keying modulation for digital optical communications," *IEEE Trans. Commun.*, vol. 43, no. 2/3/4, pp. 1591–1602, Feb./Mar./Apr. 1995.
- [7] L. Beygi, E. Agrell, P. Johannisson, and M. Karlsson, "A novel multilevel coded modulation scheme for fiber optical channel with nonlinear phase noise," in *Proc. Global Communications Conference*, Miami, FL, Dec. 2010.
- [8] A. P. T. Lau and J. M. Kahn, "Signal design and detection in presence of nonlinear phase noise," *J. Lightw. Technol.*, vol. 25, no. 10, pp. 3008–3016, Oct. 2007.
- [9] B. P. Smith, A. Farhood, A. Hunt, F. R. Kschischang, and J. Lodge, "Staircase codes: FEC for 100 Gb/s OTN," *J. Lightw. Technol.*, 2011, to appear.
- [10] G. P. Agrawal, *Lightwave Technology*. Hoboken, NJ: Wiley-Interscience, 2005.
- [11] E. M. Ip and J. M. Kahn, "Compensation of dispersion and nonlinear impairments using digital backpropagation," *J. Lightw. Technol.*, vol. 26, no. 20, pp. 3416–3425, Oct. 2008.
- [12] —, "Fiber impairment compensation using coherent detection and digital signal processing," *J. Lightw. Technol.*, vol. 28, no. 4, pp. 502–519, Feb. 2010.
- [13] G. P. Agrawal, *Nonlinear Fiber Optics*. New York, NY: Elsevier Science & Technology, 2006.
- [14] O. V. Sinkin, R. Holzlohner, J. Zweck, and C. R. Menyuk, "Optimization of the split-step Fourier method in modeling optical-fiber communication systems," *J. Lightw. Technol.*, vol. 21, no. 1, pp. 61–68, Jan. 2003.
- [15] G. Ungerboeck, "Channel coding with multilevel/phase signals," *IEEE Trans. Inf. Theory*, vol. 28, no. 1, pp. 55–67, Jan. 1982.
- [16] U. Wachsmann, R. F. H. Fischer, and J. B. Huber, "Multilevel codes: Theoretical concepts and practical design rules," *IEEE Trans. Inf. Theory*, vol. 45, no. 5, pp. 1361–1391, Jul. 1999.
- [17] G. Caire, G. Taricco, and E. Biglieri, "Bit-interleaved coded modulation," *IEEE Trans. Inf. Theory*, vol. 44, no. 3, pp. 927–946, May 1998.
- [18] G. D. Forney Jr., "Trellis shaping," *IEEE Trans. Inf. Theory*, vol. 38, no. 2, pp. 281–300, Mar. 1992.